The angular momentum of light: Optical spanners and the rotational frequency shift

Article *in* Optical and Quantum Electronics · January 1999

DOI: 10.1023/A:1006911428303

2 authors:

Miles John Padgett
University of Glasgow
782 PUBLICATIONS **58,596** CITATIONS

SEE PROFILE

Les Allen
University of Strathclyde
155 PUBLICATIONS **26,113** CITATIONS

SEE PROFILE

Optical and Quantum Electronics **31** *(1999) 1–12*

TUTORIAL REVIEW

The angular momentum of light: optical spanners and the rotational frequency shift

M. J. PADGETT, L. ALLEN
The School of Physics and Astronomy, The University of St Andrews, Fife, UK

An introduction is given to the concepts of the spin and orbital angular momentum of light beams. Both spin and orbital angular momentum can be transferred from a light beam to particles held within optical tweezers, so forming an optical spanner. Each also give rise to a frequency shift when the light beam is rotated. This arises because quarter or half-wave plates and $\pi/2$ or π mode converters play equivalent roles for spin and orbital angular momentum respectively.

1. The angular momentum of light

In 1936 Beth observed the transfer of angular momentum to a birefringent half-wave plate from a beam of circularly polarized light emitted by a tungsten bulb [1]. The wave plate was held in an evacuated cell and suspended from a quartz fibre. After transmission through the half-wave plate the sense of circular polarization was reversed. By careful measurement of the torque on the suspension, exploiting the torsional resonances, Beth was able to verify that each quantum, or photon, of circularly polarized light possessed an spin angular momentum, σ, along the propagation direction of the beam of $\hbar$. The angular momentum associated with polarisation arises from the intrinsic spin of the photon.

Less recognized is the fact that a light beam may have an orbital angular momentum. It has been understood for a long time that individual photons involved in multipole radiation must carry off orbital angular momentum [2–4]. Conservation of angular momentum frequently leads to individual photons carrying off orbital angular momentum in radiative decay; this is common in nuclear physics. However, Biedenhahn and Louck warn that

> 'multipole fields for a given value of the total angular momentum....do not have....a definite value of the orbital angular momentum'.

Consequently, although the concept of a light field possessing orbital angular momentum has long been recognized, it was not until 1992 that Allen and co-workers showed that it was possible to have an intense, experimentally realizable, light beam [5] with a unique orbital angular momentum along the beam axis. Within the paraxial approximation they showed that any monochromatic beam with an azimuthal phase dependence of $\exp(il\phi)$

was predicted to possess an orbital angular momentum equivalent to $l\hbar$ per photon. This is very similar to the way the azimuthal phase component of a quantum mechanical wavefunction is interpreted as an orbital angular momentum.

As the beams can also be polarized this means that both spin and orbital angular momentum have well defined components in the direction of the beam. Consequently, the total angular momentum of such a beam when circularly polarized, $J_z\hbar$, where

$$J_z = L_z + S_z = l + \sigma$$

This was subsequently confirmed for a solution of the full Maxwell's equations, except that there is now a very small correction term which is only zero for linearly polarized light [6]. It follows that for a linearly polarized beam with an azimuthal phase $\exp(\mathrm{i}l\phi)$, there is always a defined component of orbital angular momentum along the beam.

The $\exp(\mathrm{i}l\phi)$ phase structure produces helical wavefronts, a spiralling Poynting vector [7] and a phase singularity on the axis of the beam. This phase singularity gives rise to a characteristic intensity null on the axis of the beam. Figure 1 illustrates the difference between plane and helical wavefronts. Although such beams, often said to possess optical vortices, had been studied previously by a number of groups [8–11], none recognized their angular momentum properties. Despite the fact that this orbital angular momentum appears as an integer multiple of the number of photons in the beam it may, as with polarization, be understood purely in terms of the electromagnetic fields and associated Poynting vector. More general phase structures lead to arbitrary and non-integer values of orbital angular momentum [12].

2. Production of beams with an azimuthal phase structure and orbital angular momentum

Usually, continuous-wave lasers oscillate in a well-defined transverse mode the field distribution of which is described best by the product of a Gaussian and a pair of Hermite polynomials [13]. The Hermite–Gaussian modes form a complete basis set and so can be used to describe any arbitrary field distribution. Such modes are structurally stable. That

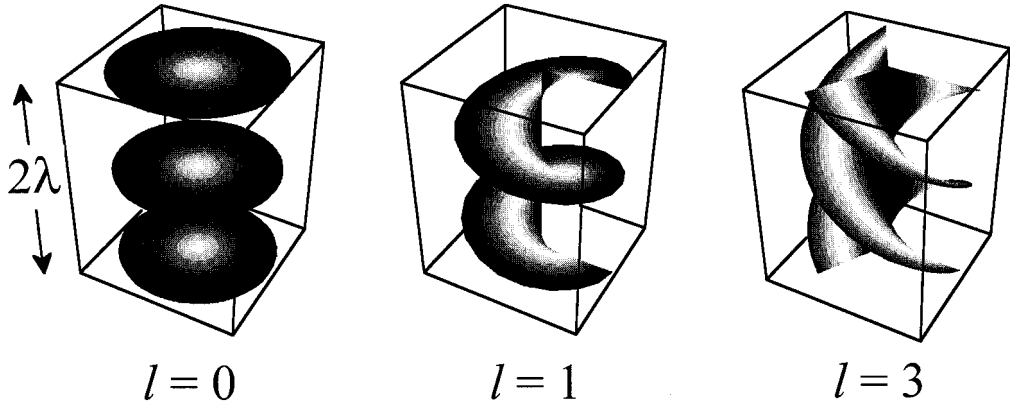

Figure 1 Wavefronts corresponding to a plane wave and two helical wavefronts which arise from the $\exp(\mathrm{i}l\phi)$ azimuthal phase term. The corresponding orbital angular momentum is $l\hbar$ per photon.

is, if radial scaling is ignored, their relative amplitude and phase remains constant as the beam propagates into the far-field. However they have spherical wavefronts and the absence of any azimuthal phase component means that no orbital angular momentum is associated with them.

Beams with helical wavefronts are also solutions of the paraxial wave equation and so can propagate in free-space. The $\exp(\mathrm{i}l\phi)$ phase term within the analytic form of the Laguerre–Gaussian beam amplitude, makes them a useful base set for the description of such beams. The analytic form of their amplitude is,

$$u(r,\phi,z) \propto \frac{z_{\mathrm{R}}}{\left(z_{\mathrm{R}}^2+z^2\right)}\left[\frac{r2^{1/2}}{w(z)}\right]^l L_p^l\left[\frac{2r^2}{w^2(z)}\right]\exp\left(\frac{-r^2}{w^2(z)}\right) \times \exp\left(\frac{-\mathrm{i}kr^2z}{2\left(z^2+z_{\mathrm{R}}^2\right)}\right)\exp(-\mathrm{i}l\phi)\exp\left(\mathrm{i}(2p+l+1)\tan^{-1}\frac{z}{z_{\mathrm{R}}}\right)$$

where L_p^l is a Laguerre polynomial, $w(z)$ the radius of the beam at position z and z_{R} the Rayleigh range. It may be seen that in addition to the azimuthal mode index, l, there is a second mode index, p, which describes the number of radial nodes in the field. As with the Hermite–Gaussian modes, the Laguerre–Gaussian modes are structurally stable with propagation. Although lasers have been configured to produce Laguerre–Gaussian beams directly [14, 15], the inherent symmetry in most laser systems makes it difficult to favour one helical wavefront handedness over the other. It is therefore usual to generate Laguerre–Gaussian beams by the conversion of Hermite–Gaussian beams external to the laser cavity, where the symmetry can be broken more easily.

One method of generating beams with helical wavefronts uses computer generated holograms [16, 17]. These holograms usually take the form of a diffraction grating with a period, D, containing l dislocations at the centre of the hologram. The detailed form of the hologram for $l = 1$ is shown in Fig. 2 and is simply the interference pattern formed when a plane wave crosses a beam with a helical phase structure. The boundaries between the dark and light areas of the hologram are given by,

$$l\frac{\phi}{\pi} = n + \frac{2r}{D}\cos\phi$$

where n is a series of integers $\ldots -3, -2, -1, 0, 1, 2, 3, \ldots$

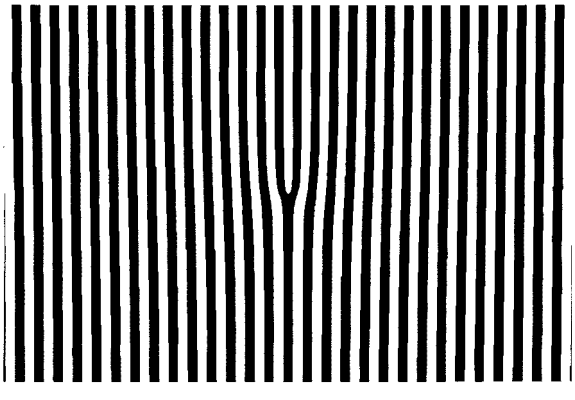

Figure 2 A computer generated hologram which when illuminated by a beam with a plane wavefront gives diffracted beams with helical wavefronts.

If a fundamental Gaussian beam from a conventional laser is aligned with the centre of the hologram, the first order diffracted beam has a $\exp(il\phi)$ phase structure and a detailed mode analysis shows that nearly 80% of the first order energy lies in the single-ringed $p = 0$ mode. Recently, the inclusion of a radial phase reversal in the grating pattern has extended this technique to the generation of multi-ringed $p > 0$ modes [18]. The use of holograms to generate Laguerre–Gaussian modes has two limitations. First, even the best holograms which are blazed to favour one particular diffracted order are only 60% efficient. Second, the resulting beam is not a single Laguerre–Gaussian mode but rather a composition of various modes all with the same azimuthal mode index, l, but differing radial indices, p.

In 1993, following initial work by Tamm and Weiss [14] and Abramochkin and Volostnikov [19], Beijersbergen *et al.* [20] reported a method which used cylindrical lenses to generate pure Laguerre–Gaussian beams with any mode indices. A pair of identical cylindrical lenses may be shown to introduce different Gouy phase shifts between astigmatically focused Hermite–Gaussian modes, such that the resultant mode is a pure Laguerre–Gaussian. The simplest case to understand is the transformation of a Hermite–Gaussian $m = 1, n = 0\,(HG_{10})$ mode into the corresponding Laguerre–Gaussian mode. A HG_{10} mode, aligned at 45° to the axes of the lenses can be expressed as two in-phase HG_{10} modes orthogonal to each other and aligned with the principal axes of the lenses. The separation of the cylindrical lenses is arranged such that these two orthogonal modes undergo Gouy phase shifts [13] that differ by 90°. The two modes combine after the lenses to give a Laguerre–Gaussian field distribution with $l = 1$ and $p = 0$. This is a single-ringed annular beam with a well-defined azimuthal phase structure of $\exp(i\phi)$, see Fig. 3. In the case of the cylindrical lens mode converter, any incident Hermite–Gaussian mode of indices n and m is converted into a single Laguerre–Gaussian mode with $l = n - m$ and $p = \min(m, n)$. Figure 4 shows for a selection of Hermite–Gaussian modes, the corresponding Laguerre–Gaussian modes and the interference pattern obtained between the Laguerre–Gaussian modes and a plane wave [21]. The spiral fringes show clearly the azimuthal phase term associated with the helical wavefronts. We may note that for $n = m = 3$ that $l = 0$ and there is no orbital angular momentum and, unlike the other examples shown, there is an on-axis intensity. The cylindrical lens mode converter is, in principle, 100% efficient and produces pure Laguerre–Gaussian modes. The 90° phase shift introduced between orthogonal Hermite–Gaussian modes leads this arrangement of cylindrical lenses to be described as a $\pi/2$ converter and so is analogous to a quarter-wave plate. For spin angular momentum, a quarter-wave plate transforms linearly polarized light into circularly polarized light, while for orbital angular momentum, the $\pi/2$ converter transforms a spherical wavefront into a helical wavefront. It is possible to design a π converter based on cylindrical lenses which reverses the sense of the helical wavefronts analogous to the way a half-wave plate reverses the sense of the circular polarization [20].

Other methods for generating beams with helical wavefronts have also been reported; these include spiral phase plates [22] which introduce an azimuthal phase term to the transmitted beam and stressed fibres [23] which work in a similar way to the cylindrical lens converter. The spiral phase plate technique has also been extended to the mm-wave region of the spectrum [24], where the longer wavelength gives an increased orbital angular momentum per unit power in the beam. The spiral phase plate has a step discontinuity of depth s such that,

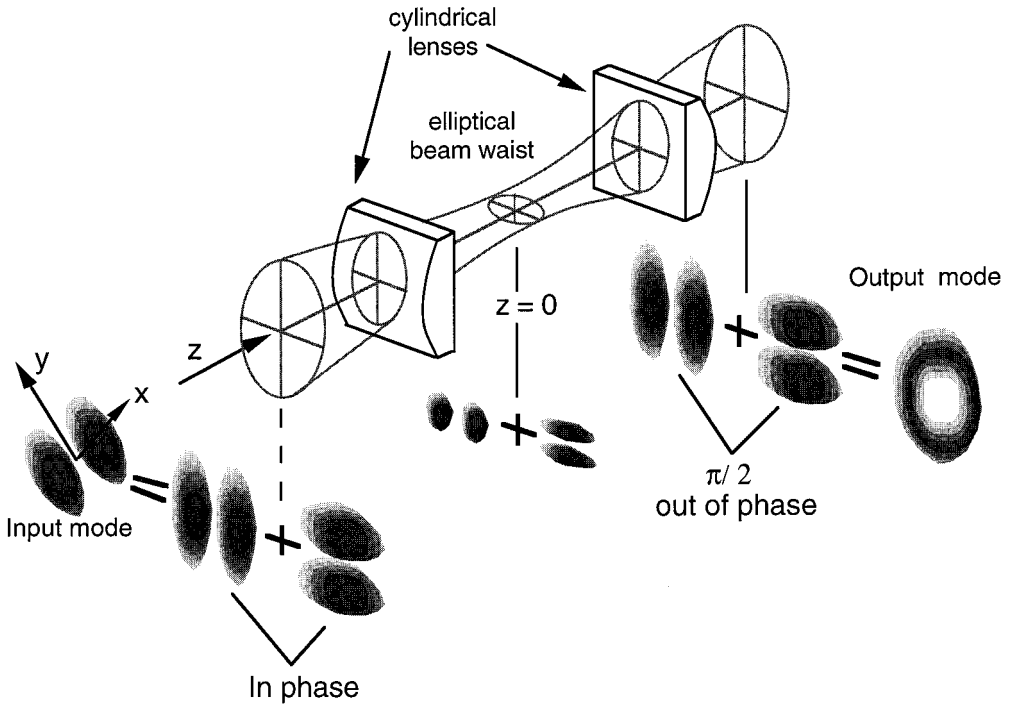

Figure 3 The cylindrical lens mode converter for the conversion of a Hermite–Gaussian $n = l$, $m = 0$ mode into the corresponding Laguerre–Gaussian mode with $l = 1$ and $p = 0$. The lenses of focal length f are separated by $f/2^{1/2}$ where the Rayleigh range of the input beam is $(1 + 1/2^{1/2})f$.

$$s = \frac{l\hbar\lambda}{(n-1)}$$

where n is the refractive index of the plate material. It is worth noting that a simple geometric optics analysis of the interaction of the spiral phase plate with a light ray shows that angular momentum transferred is indeed $l\hbar$ per photon [24].

3. Optical tweezers for the manipulation of micron sized particles

In 1987, after more than a decade of related research, Ashkin and co-workers used a tightly focused beam of laser light to trap a glass sphere in three dimensions [25]. This technique is now commonly referred to as optical tweezers and is widely used in many biological applications. These include measuring the compliance of bacterial tails [26] the measurement of the forces exerted by single muscle fibres [27] and the stretching of single strands of DNA [28].

Optical tweezers rely on the extremely large gradient in the electric field generated in the region of a tightly focused laser beam. Any dielectric particle in the vicinity of the focus experiences a force directed towards the region of highest field. At optical frequencies, a dielectric material is one which has a predominately real refractive index. Hence, optical tweezers usually only work for transparent particles. If the laser beam is focused tightly enough then the 'gradient force' can be greater than that due to gravity and the particle

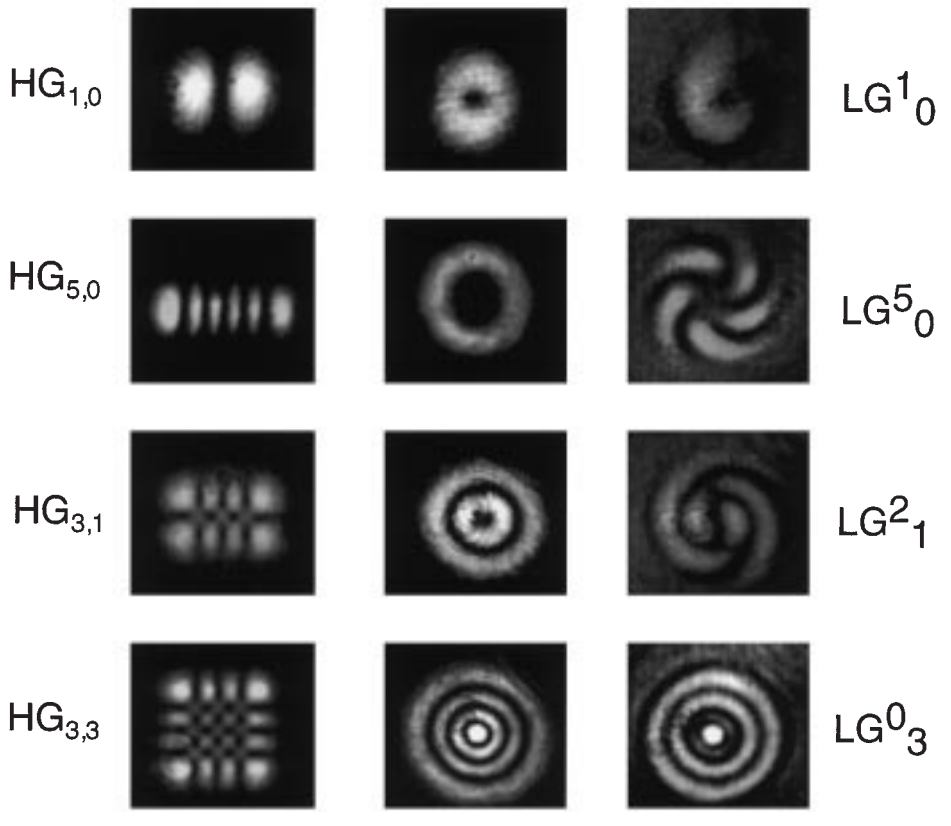

Figure 4 A selection of Hermite–Gaussian modes, the corresponding Laguerre–Gaussian modes produced by the cylindrical lens mode converter and the interference pattern between the Laguerre–Gaussian mode and a plane wave, illustrating the azimuthal phase structure. The number of arms of the spiral is equal to *l*.

becomes trapped in three dimensions. For transparent particles a few microns in diameter, suspended in water or alcohol, a few milliwatts of laser power focused with an oil-immersion microscope objective is sufficient to form a robust trap [29]. Lateral and axial forces of a few hundred *pN* can be generated which allows particles to be manipulated at speeds of tens of microns per second.

4. The transfer of angular momentum between light and matter

By causing a wave plate to rotate, Beth not only demonstrated that the spin angular momentum content of circularly polarized light could be transferred to a macroscopic object, but also that it was indeed $\hbar$ per photon. The identification of beams with orbital angular momentum theoretically predicted to have $l\hbar$ per photon led to ideas as to how this could be experimentally confirmed. To do so, it is important to analyse the mechanisms by which angular momentum can be transferred. Linearly polarized light is transformed into circularly polarized light using a birefringent quarter-wave plate. Conservation of angular momentum dictates that any change in angular momentum to the light is equal and opposite to the change in angular momentum to the wave plate. Similarly, the transformation of a Hermite–Gaussian mode into a Laguerre–Gaussian mode

will result in a transfer of angular momentum to the mode converter. Another, more obvious mechanism for the transfer of both spin and orbital angular momentum of the light is absorption. When the light is absorbed, or partially absorbed, both spin and orbital angular momentum are transferred to the absorber with equal efficiency. However, care must be taken when interacting light beams with suspended optical components. If the light beam is not coaxial with the suspension axis, the linear momentum content of the beam of h/λ per photon will give rise to an additional torque on the optical component. In 1994, we suggested an alternative to suspending the optical element [30]. By using a Laguerre–Gaussian within an optical tweezers, the need for a separate suspension mechanism is removed. The laser light itself acts to hold the interacting particle on the beam axis.

The first observation of the transfer of orbital angular momentum to a particle was reported by Rubinsztein-Dunlop and co-workers in 1995 [31]. They holographically generated a $l = 3$ helical beam and used it to trap absorbing ceramic powder. The absorbing nature of the particles meant that rather than being held at the focus of the beam, the particles were optically held in two dimensions within the on-axis intensity minimum of the beam. The absorption of the light and the associated linear momentum, resulted in a force in the propagation direction of the laser beam and the restraint in the third dimension was provided by the microscope slide. They observed a rotation of the ceramic particle which they attributed to the absorption of the orbital angular momentum from the light beam.

The successful demonstration of a true optical tweezers using a Laguerre–Gaussian mode for the trapping and rotation of partially absorbing Teflon particles suspended in alcohol was reported in 1996 [32]. The use of particles which absorbed only a few percent of the incident laser light meant that the gradient force was sufficient to overcome the force associated with the linear momentum and consequently the particles were trapped in three dimensions. These trapped Teflon particles were observed to rotate at several Hertz, hence the term 'optical spanner'.

The rotation speed may be compared with predictions made on the basis of the estimated absorption of the light and the viscous drag of the surrounding fluid. However, the errors inherent in this approach make the quantification of the orbital angular momentum extremely difficult. A more meaningful measurement is to compare the orbital angular momentum directly with the spin angular momentum. Using a circularly polarized Laguerre–Gaussian mode with $l = 1$, the handedness of the polarization can be set to give a total angular momentum of the light beam, spin plus orbital, of $\hbar + \hbar = 2\hbar$ or $\hbar - \hbar = 0$ per photon. The observed start/stop nature of the rotation confirms that the orbital angular momentum associated with a $l = 1$ Laguerre–Gaussian mode is $\hbar$ per photon [33]. Figure 5 shows successive frames of video demonstrating the start/stop behaviour of the trapped particle. This experiment confirms that both the spin and orbital angular momentum of light can be transferred to a macroscopic object in an equivalent fashion. A complementary experiment was also performed using a $l = 3$ Laguerre–Gaussian mode showing that the rotation speed could be increased or decreased by making the light circularly polarized [34].

5. The rotational frequency shift

Nearly 20 years ago Garetz and Arnold demonstrated that the frequency of a circularly polarized light beam could be shifted by passing it through a rotating half-wave plate [35].

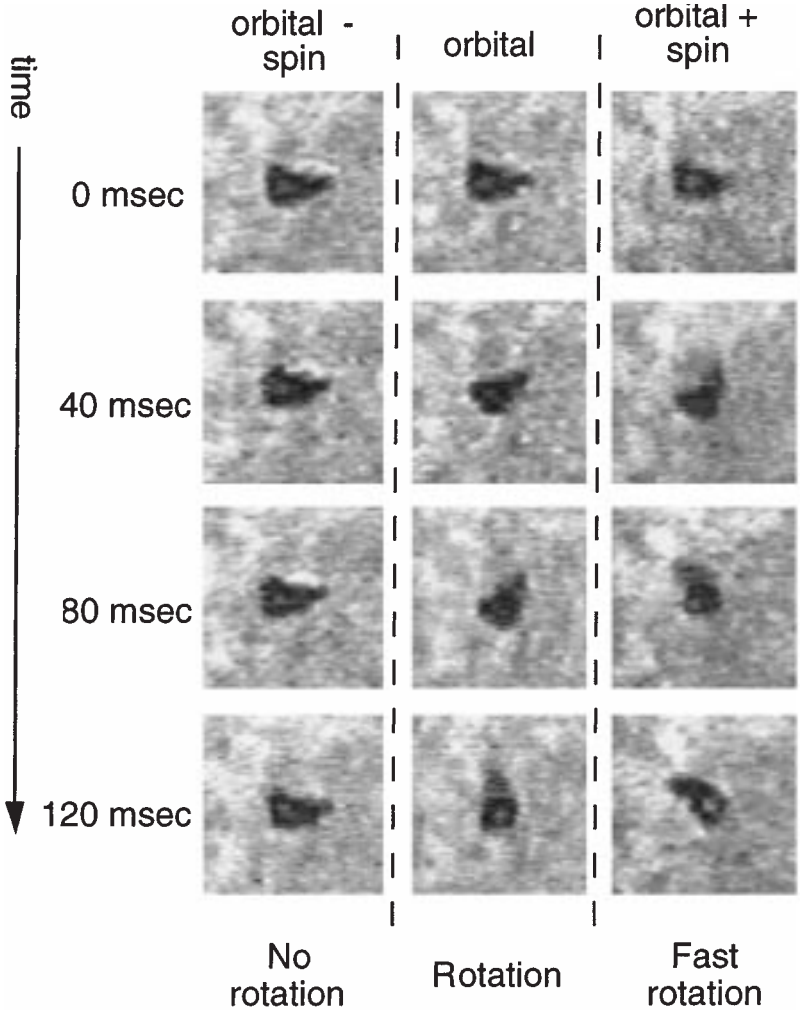

Figure 5 Successive frames of a video showing that the spin and orbital angular momentum terms can be added to give faster rotation, or subtracted to give no rotation, in an optical spanner.

The frequency shift imparted to the light beam is equal to twice the rotation frequency of the wave plate. An analysis of this interaction with Jones Matrices shows that the rotating half-wave plate rotates the linear polarization of the transmitted beam at twice the rotation frequency of the wave plate. For a circularly symmetric beam, the rotation of the polarization can be considered to be a rotation of the beam as a whole. Consequently, the frequency shift can be seen to be equal to the rotation frequency of the beam.

More recently, Nienhuis predicted that a Laguerre–Gaussian beam with its associated orbital angular momentum should experience a frequency shift equal to twice the rotational frequency of a rotating π converter [36]. As already discussed, a stationary π converter reverses the sense of the helical wavefronts in an equivalent way to a stationary half-wave plate reversing the sense of circular polarization. Although the π converter we

have described consists of two cylindrical lenses, it is clear that it can also be made using a Dove prism, the single internal reflection of which inverts any transmitted beam. Dove prisms are frequently used as image rotators where the rotational frequency of the image is twice that of the prism. In other words a rotating half-wave plate rotates the polarization of the beam whereas a rotating π converter rotates the phase/amplitude structure of the beam [20].

We believe both of these effects to be examples of the rotational frequency shift highlighted recently by Bialynicki-Birula and Bialynicka-Birula [37]. They stress that this shift should not be confused with the Doppler shift observed for rotating objects which is due to the rotation having a linear velocity with respect to the observer. Unlike the linear Doppler shift which is maximal in the plane of rotation, their effect is maximal in the direction of the angular velocity vector where the linear Doppler shift is zero. Their prediction can be interpreted as a frequency shift equal to the rotation frequency of the light beam, Ω, multiplied by the angular momentum per photon in units of $\hbar$.

By use of Laguerre–Gaussian beams with $l = 0, 1, 2, 3$ in the mm-wave region of the spectrum and a rotating π converter based on a Dove prism, the rotational frequency shift for a Laguerre–Gaussian beam has been successfully measured [38]. The experiment was configured as a Mach–Zehnder interferometer with a rotating Dove prism in one arm and a stationary one in the other, see Fig. 6. The frequency shift was deduced from the beat frequency measured at the exit port of the interferometer and confirms that the frequency shift is equal to twice the rotational frequency of the π converter multiplied by the angular momentum per photon, l. It appears that if both the polarization and phase structure of the beam are rotated at a angular frequency Ω, then the total frequency shift, $\Delta\omega$, is given by $\Delta\omega = (l + \sigma)\Omega = J_z\Omega$.

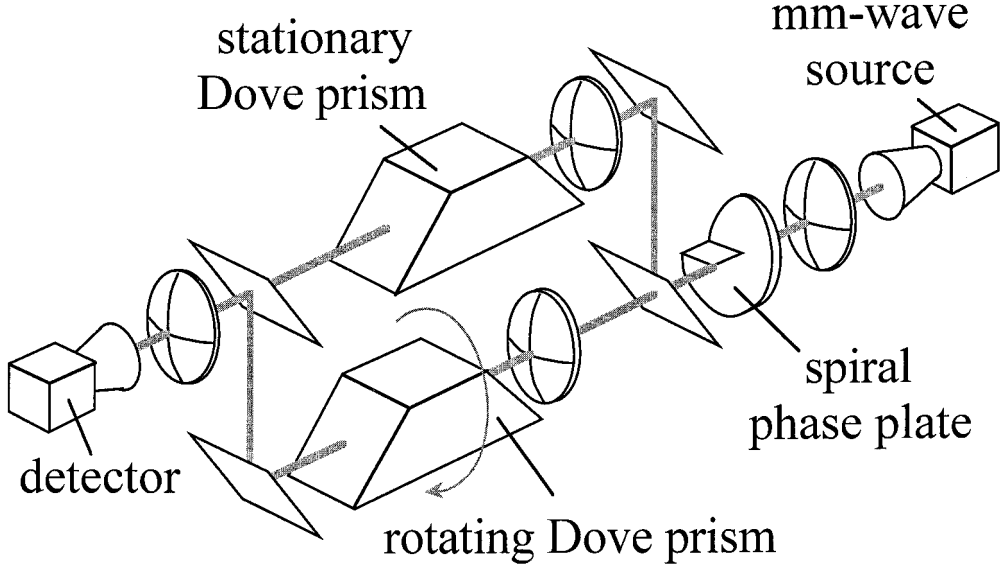

Figure 6 Mach–Zehnder interferometer with a rotating Dove prism in one arm, for the observation of the rotational frequency shift of a beam possessing orbital angular momentum.

6. Conclusions

In this review, we have stressed that the angular momentum of light beams has two distinct contributions. Spin angular momentum is an intrinsic property of the photon and for circularly polarized light is $\pm\hbar$ per photon. In contrast, the orbital angular momentum is associated with the phase structure of the beam and, for a helical wavefront with a $\exp(\mathrm{i}l\phi)$ phase term, is equal to $l\hbar$ per photon. Circularly polarized light may be produced from linearly polarized laser light by means of a birefringent quarter-wave plate. Orbital angular momentum may be produced by use of a $\pi/2$ mode converter which modifies the phase structure of the beam.

Absorption of the light allows both the spin and orbital angular momentum of a light beam to be transferred to macroscopic objects held within optical tweezers, forming an optical spanner. In addition, when the light beam is rotated, the orbital angular momentum results in a frequency shift in an analogous fashion to spin angular momentum. This is because quarter- or half-wave plates and a $\pi/2$ or π mode converters play equivalent roles for spin and orbital angular momentum respectively (see Fig. 7).

The article has deliberately concentrated on areas where the spin and orbital angular momentum have analogous behaviour. In other areas such as non-linear optics or interactions with atomic or ionic systems the situation is more complicated. For example,

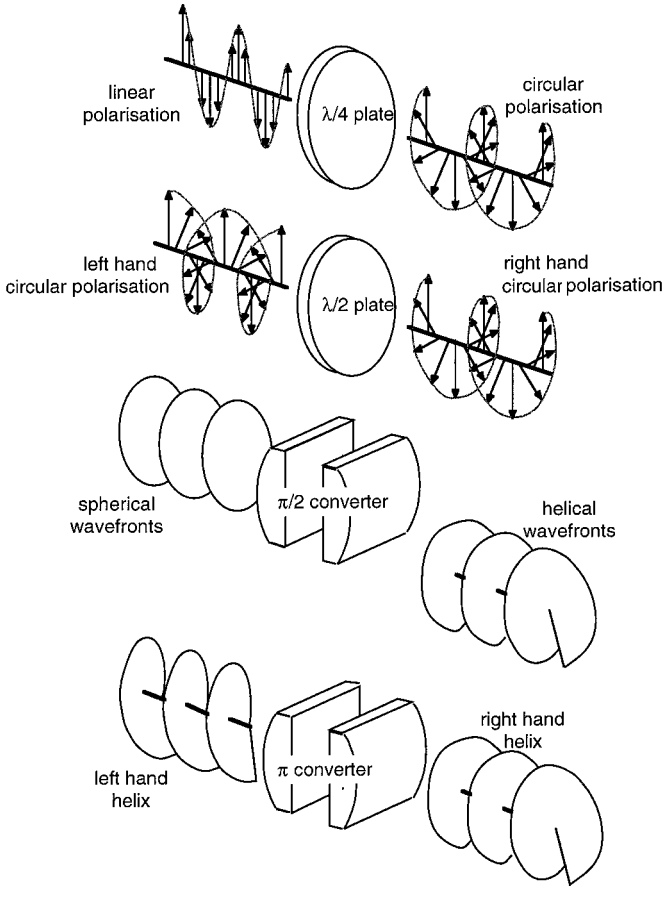

Figure 7 Quarter or half-wave plates and $\pi/2$ and π mode converters play equivalent roles for spin and orbital angular momentum respectively.

within non-linear optics the orbital angular momentum is not exchanged with the non-linear material but is conserved within the light beam alone, which leads to a mode transformation [39, 40]. For the excitation of atomic dipole transitions, the polarization state of the beam selects which transitions are allowed. The principal effect of the helical wavefronts and the associated orbital angular momentum is to Doppler shift the transition frequencies and induce gross motion in the atoms or ions [41, 42].

Acknowledgements

We would like to thank the significant contribution made by K.D. Dholakia, N.B. Simpson, J. Courtial and J. Arlt to much of the work reported in this review. MJP is a Royal Society Research Fellow. This work has been supported by the EPSRC.

References

1. R. E. BETH, *Phys. Rev.* **10** (1936) 115.
2. J. D. JACKSON, *Classical Electrodynamics* (Wiley, New York, 1962).
3. M. E. ROSE, *Multipole Fields* (Wiley, New York, 1955).
4. L. C. BIEDENHAHN and J. D. LOUCK, Angular momentum in quantum physics. In *Encyclopaedia of Mathematics and Its Applications*, Vol. VIII (Addison-Wesley, New York, 1962).
5. L. ALLEN, M. W. BEIJERSBERGEN, R. J. C. SPREEUW and J. P. WOERDMAN, *Phys. Rev. A* **45** (1992) 8185.
6. S. M. BARNETT and L. ALLEN, *Opt. Commun.* **110** (1994) 670.
7. M. J. PADGETT and L. ALLEN, *Opt. Commun.* **121** (1995) 36.
8. J. M. VAUGHAN and D. V. WILLETTS, *Opt. Commun.* **20** (1979) 263.
9. C. TAMM, *Phys. Rev. A* **38** (1988) 5960.
10. V. YU. BAZHENOV, M. V. VASNETSOV and M. S. SOSKIN, *JEPT Lett.* **52** (1991) 429.
11. A. G. WHITE, C. P. SMITH, N. R. HECKENBERG, H. RUBINSZTEIN-DUNLOP, R. MCDUFF, C. O. WEISS and C. TAMM, *J. Mod. Opt.* **38** (1991) 2531.
12. J. COURTIAL, K. DHOLAKIA, L. ALLEN and M. J. PADGETT, *Opt. Commun.* **144** (1997) 210.
13. A. E. SIEGMAN, *Lasers* (University Science Books, Mill Valley, CA, 1986).
14. C. TAMM and C. O. WEISS, *J. Opt. Soc Am. B* **7** (1990) 1034.
15. M. HARRIS, C. A. HILL, P. R. TAPSTER and J. M. VAUGHAN, *Phys. Rev. A* **49** (1994) 3119.
16. N. R. HECKENBERG, R. MCDUFF, C. P. SMITH and A. G. WHITE, *Opt. Lett.* **17** (1992) 221.
17. N. R. HECKENBERG, R. MCDUFF, C. P. SMITH, H. RUBINSZTEIN-DUNLOP and M. J. WEGENER, *Opt. Quantum Electron* **24** (1992) S951.
18. J. ARLT, K. DHOLAKIA, L. ALLEN and M. J. PADGETT, *J. Mod. Opt.* **45** (1998) 1231.
19. E. ABRAMOCHKIN and V. VOLOSTNIKOV, *Opt. Commun.* **83** (1991) 123.
20. M. W. BEIJERSBERGEN, L. ALLEN, H. E. L. O. VAN DER VEEN and J. P. WOERDMAN, *Opt. Commun.* **96** (1993) 123.
21. M. PADGETT, J. ARLT, N. SIMPSON and L. ALLEN, *Am. J. Phys.* **64** (1996) 77.
22. M. W. BEIJERSBERGEN, R. P. C. COERWINKEL, M. KRISTENSEN and J. P. WOERDMAN, *Opt. Commun.* **112** (1994) 321.
23. D. MCGLOIN, N. B. SIMPSON and M. J. PADGETT, *Appl. Opt.* (accepted for publication).
24. G. A. TURNBULL, D. A. ROBERTSON, G. M. SMITH, L. ALLEN and M. J. PADGETT, *Opt. Commun.* **127** (1996) 183.
25. A. ASHKIN, J. M. DZIEDZIC, J. E. BJORKHOLM and S. CHU, *Opt. Lett.*, **11** (1986) 288.
26. S. M. BLOCK, D. BLAIR and H. C. BERG, *Nature* **388** (1989) 514.
27. J. T. FINER, R. M. SIMMONS, J. A. SPUDICH, *Nature* **368** (1994) 113.
28. M. D. WANG, H. YIN, R. LANDICK, J. GELLES and S. M. BLOCK, *Biophys. J.* **72** (1997) 1335.
29. H. FELGNER, O. MÜLLER and M. SCHLIWA, *Appl. Opt.* **34** (1995) 977.
30. M. J. PADGETT, and L. ALLEN, at the *Rank Prize Mini-Symposium on Optical Tweezers*, August 1994; quoted by B. Amos and P. Gill, Meas., *Optical Tweezers Meas. Sci. Technol.* **6** (1995) 248.
31. H. HE, M. E. J. FRIESE, N. R. HECKENBERG and H. RUBINSZTEIN-DUNLOP, *Phys. Rev. Lett.* **75** (1995) 826.
32. N. B. SIMPSON, L. ALLEN and M. J. PADGETT, Optical spanners. In *Inaugural Meeting of the Scottish Chapter of LEOS*, Glasgow University, Glasgow, 1996.

33. N. B. SIMPSON, K. DHOLAKIA, L. ALLEN and M. J. PADGETT, *Opt. Lett.* **22** (1997) 52.
34. M. E. FRIESE, J. ENGER, H. RUBINSZTEIN-DUNLOP and N. R. HECKENBERG, *Phys. Rev. A* **54** (1996) 1593.
35. B. A. GARETZ and S. ARNOLD, *Opt. Commun.* **31** (1979) 1.
36. G. NIENHUIS, *Opt. Commun.* **132** (1996) 8.
37. I. BIALYNICKI-BIRULA and Z. BIALYNICKA-BIRULA, *Phys. Rev. Lett.* **78** (1997) 2539.
38. J. COURTIAL, K. DHOLAKIA, D. ROBERTSON, L. ALLEN and M. J. PADGETT, *Phys. Rev. Lett.* **80** (1998) 3217.
39. K. DHOLAKIA, N. B. SIMPSON, M. J. PADGETT and L. ALLEN, *Phys. Rev. A* **54** (1996) R3742.
40. J. COURTIAL, K. DHOLAKIA, L. ALLEN and M. J. PADGETT, *Phys. Rev. A* **56** (1997) 4193.
41. M. BABIKER, W. L. POWER and L. ALLEN, *Phys. Rev. Lett.* **73** (1994) 1239.
42. L. ALLEN, M. BABIKER, W. K. LAI and V. E. LEMBESSIS, *Phys. Rev. A* **54** (1996) 4259.